

PAPER • OPEN ACCESS

## Analysis on ductility and energy dissipation performance of steel box column-beam irregular joint

To cite this article: Zongbo Hu 2019 *IOP Conf. Ser.: Earth Environ. Sci.* **218** 012046

View the [article online](#) for updates and enhancements.



**IOP | ebooks™**

Bringing you innovative digital publishing with leading voices to create your essential collection of books in STEM research.

Start exploring the collection - download the first chapter of every title for free.

# Analysis on ductility and energy dissipation performance of steel box column-beam irregular joint

Zongbo Hu<sup>1\*,2</sup>

<sup>1</sup> Institute of Equipment Management and Support, Engineering University of People's Armed Police Force, Xi'an, Shanxi, 710086, China

<sup>2</sup> School of Civil Engineering, Xi'an University of Architecture and Technology, Xi'an, Shanxi, 710055, China

\*Corresponding author's e-mail: huzongbo\_1985@163.com

**Abstract.** Through quasi-static test of six different steel box column-beam irregular joint models, the behaviors including the axial load level and columns stiffness level, the hysteretic curve, failure mechanism were analyzed. Some mechanical performances of steel irregular joint such as ductility, ultimate bearing capacity, energy dissipation were studied. The results indicate that the steel box column-beam irregular joint has good seismic performance and energy dissipation capacity. The ductility coefficient is between 2.02 and 2.66, satisfying the requirements of plastic ultimate deformation. Steel irregular joint has stronger energy dissipation capacity. Energy dissipation in the small core area of panel zone plays key roles in energy dissipation of the specimen. It is helpful for further study of the mechanical performance of the steel box column-beam irregular joint.

## 1. Introduction

With the development of national economy, all kinds of steel structure has been more widely used in our country, and the development of large garment and large-span steel structure is the main trend. In many complex industrial and civil building structure, a lot of irregular joints are appeared. An irregular joint is defined as a joint with a beam of variable cross-section and/or a column of variable cross-section.

By the variation of the beam and column section form, the force mechanism and deformation characteristics of normal joints are obviously different with irregular joints. At present, considerable research is focused on traditional steel beam-column joints compared with steel irregular joints[1-4]. In this paper, through quasi-static test of six different steel box column-beam irregular joint models, ductility and energy dissipation performance of steel irregular joint were studied.

## 2. Test survey

Based on the irregular joints of the steel main workshop in a power plant, test specimens at 1/4 scale of were designed for use in a prototype model. There were two series of six cruciform joints, the JD20 series and the JD27 series. Around a joint were an identical box column but different beams, an I-shaped beam and a box beam. Welded flange and bolted web connections were used to connect the I-shaped beam and the box column; fully welded connections were used to connect the box beam and the box column.



To study the ductility and energy dissipation performance of the panel zone, specimens were made according to the different axial compression and beam height ratios[5]. Additionally, the axial compression ratios of three specimens in each series were 0.2, 0.3 and 0.4, and the design axial forces were, respectively, 540kN, 800kN and 1050kN. This test adopts quasi-static loading with the test setup illustrated in Fig. 1, and the materials performance of specimens shown in Table 1.

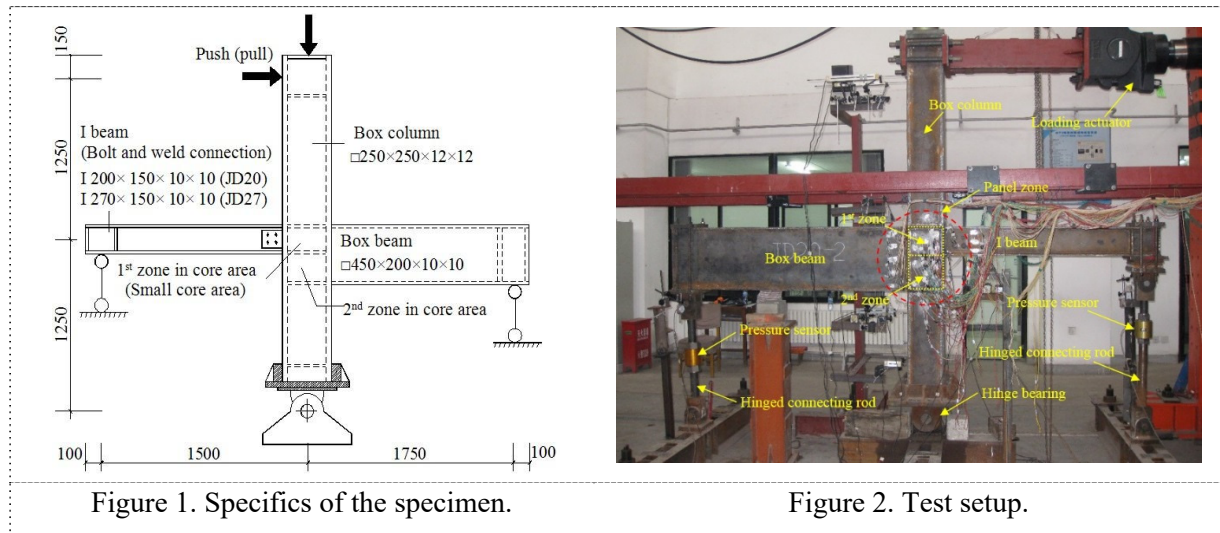


Figure 1. Specifics of the specimen.

Figure 2. Test setup.

Table 1. Materials performance of steel.

Plate thickness /mm	Elasticity modulus $E/10^5\text{MPa}$	Yield stress $f_y/\text{MPa}$	Yield strain $\epsilon_y/\mu\epsilon$	Ultimate stress $f_u/\text{MPa}$
6	2.02	310.54	1540	453.06
10	2.07	285.70	1390	430.99
12	2.07	286.35	1392	449.34

### 3. Test result

As shown in Fig.2, the quasi-static test have been implemented in XAUAT’s national key laboratory of structural engineering and earthquake.  $P-\Delta$  skeleton curves of the JD20 and JD27 series are shown in Fig.3. As shown in the figure, with the increase of lateral displacement, the web weld in the 2nd zone opened, so, at that moment, the box beam lower flange cannot be used to transmit tension to the panel zone, only the small core area was able to bear the shear force. Therefore, the skeleton curves of the specimens sharply decline when the load exceeds the limit. The results show that the degradation of joint stiffness is significant and the residual deformation of the panel zone is increased.

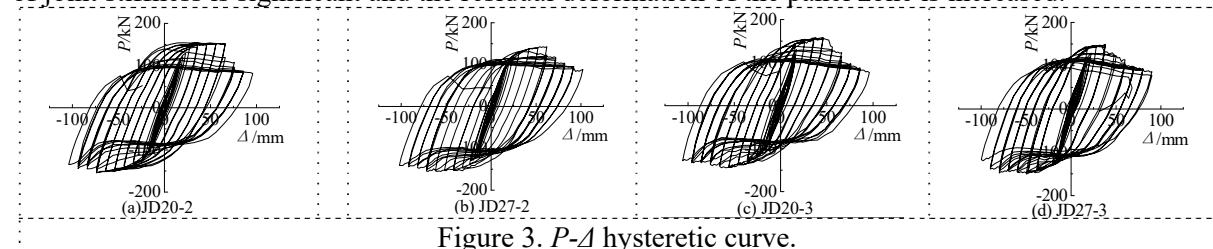


Figure 3.  $P-\Delta$  hysteretic curve.

### 4. Analysis on the performances of Lateral displacement and joint ductility

Displacement ductility coefficient and displacement angle are used to evaluate the ductility performance of joint[6]. Displacement ductility coefficient  $\mu$  is the ratio of column top horizontal displacement  $\Delta_u$  at failure and  $\Delta_y$  at yield of the joint[7]. Displacement ductility coefficient is used to

describe the ductility is good or bad. The test results including load, displacement, displacement angle and displacement ductility coefficient are shown in table 2.

Table 2. Main test results of each stage.

Joint Number	Loading Direction	Yield Point				Ultimate Point		Damage Point			$\mu = \Delta_u / \Delta_y$
		$\Delta_y / \text{mm}$	$P_y / \text{kN}$	$\varphi_y$	Elastic Drift Ratio $\varphi_y$	$\Delta_m / \text{mm}$	$P_m / \text{kN}$	$\Delta_u / \text{mm}$	$P_u / \text{kN}$	Elastic-plastic Drift Ratio $\varphi_u$	
JD20-1	Push	30.00	130.71	0.012	0.012	60.00	143.58	65.76	122.04	0.026	2.19
	Pull	-30.00	-	-0.012		-98.01	-162.89				
JD20-2	Push	28.01	144.90	0.011	0.012	56.02	152.79	70.53	129.87	0.028	2.52
	Pull	-30.02	-	-0.012		-74.01	-154.25				
JD20-3	Push	24.04	148.23	0.010	0.011	46.01	157.78	63.99	134.11	0.026	2.66
	Pull	-30.00	-	-0.012		-63.99	-144.41				
JD27-1	Push	27.99	136.74	0.011	0.012	47.98	142.83	56.63	121.41	0.023	2.02
	Pull	-34.01	-	-0.014		-82.01	-152.56				
JD27-2	Push	28.97	127.46	0.012	0.011	61.99	142.82	65.47	121.40	0.026	2.26
	Pull	-28.01	-	-0.011		-72.01	-154.55				
JD27-3	Push	24.01	141.94	0.010	0.010	38.02	149.47	50.02	127.05	0.020	2.08
	Pull	-25.00	-	-0.010		-49.97	-150.03				

As shown in table 2, the displacement ductility coefficient  $\mu$  of six joint specimens is 2.02 between 2.66, with a mean of 2.29. The displacement ductility coefficients of six joint specimens is not very big. The reason is that bearing capacity drops rapidly because of sudden fracture of the weld between steel column flange and connection web under the action of repeated horizontal load after the web of joint core area yield. Therefore, the weld quality of the panel zone is highly valued. According to the code for seismic design of buildings (GB50011-2001), the elastic interstory displacement angle  $\varphi_e$  of multi-storey and high-rise steel structure is 0.0033, elastoplastic interstory displacement angle  $\varphi_p$  is 0.02. In this test, the elastic displacement angle  $\varphi_y$  of six joint specimens is 0.010 between 0.012,  $\varphi_y$  is 3.0 to 3.63 times as much as  $\varphi_e$ . The elastoplastic interstory displacement angle  $\varphi_u$  is 0.020 between 0.028,  $\varphi_u$  is 1.0 to 1.4 times as much as  $\varphi_p$ . Obviously, all of the elastoplastic displacement angles of six joint specimens exceed stipulated limit of the code. At this moment, the degradation of bearing capacity of the structural members is not obvious. Accordingly, these steel irregular joints have good elastoplastic deformation ability. Analysis on energy dissipation performance of panel zone

#### 4.1 Horizontal displacement on the top of column caused by the shear deformation in the panel zone

The total energy dissipation of the specimens consists of three parts, namely energy dissipation of the panel zone, energy dissipation of the beam plastic hinge, and energy dissipation of the column plastic hinge[8]. Because steel irregular joint have two core area, namely 1<sup>st</sup> zone and 2<sup>nd</sup> zone. Clearly, energy dissipation of the panel zone is composed of energy dissipation in the small core area and 2<sup>nd</sup> zone. The test data and test phenomenon show that the plastic shear deformation of small core area is much greater than 2<sup>nd</sup> zone. The results indicate that energy dissipation in the small core area of panel zone plays key roles in energy dissipation of the specimen. Therefore, investigation of energy dissipation performance in small core is very important. On the premise of ignoring shear deformation of 2<sup>nd</sup> core area,  $\Delta_1$  is defined as the horizontal displacement on the top of column caused by shear deformation in the small core. Consequently, the area surrounded by P- $\Delta_1$  curve is the energy dissipation of the panel zone.

Calculation sketch of column end displacement caused by the deformation of the panel zone is shown in fig.5. The column end horizontal displacement caused by the shear deformation of the panel zone can be calculated using the following formula:

$$\Delta_1 = |SK| \times \sin \alpha_3 - |KJ| \times \sin \alpha_1 + |JT| \times \sin \alpha_3 = 2 \times \frac{H_0}{2} \times \sin \alpha_3 - h \times \sin \alpha_1 \quad (1)$$

$$\Delta_1 = H_0 \times \sin \left( \frac{L_0}{L_0 + b} \gamma \right) - h \times \sin \left( \frac{d}{L_0 + d} \gamma \right) \quad (2)$$

$$\gamma = \alpha_1 + \alpha_2 = \frac{\sin\theta \cdot \bar{X}}{b} + \frac{\cos\theta \cdot \bar{X}}{a} = \frac{\sqrt{a^2 + b^2}}{2ab} (a_1 + a_2 + b_1 + b_2) \tag{3}$$

Where  $\gamma$  is the shear angle;  $a_1$ 、 $a_2$ 、 $b_1$  and  $b_2$  are the amount of elongation or shortening on the diagonal of the core area, respectively (shown in fig.4) [9];  $L_0$  is the net span of the beam excluding small core width;  $H_0$  is the net height of the column excluding small core height;  $h$  is the height of the beam section;  $d$  is the width of the column section.

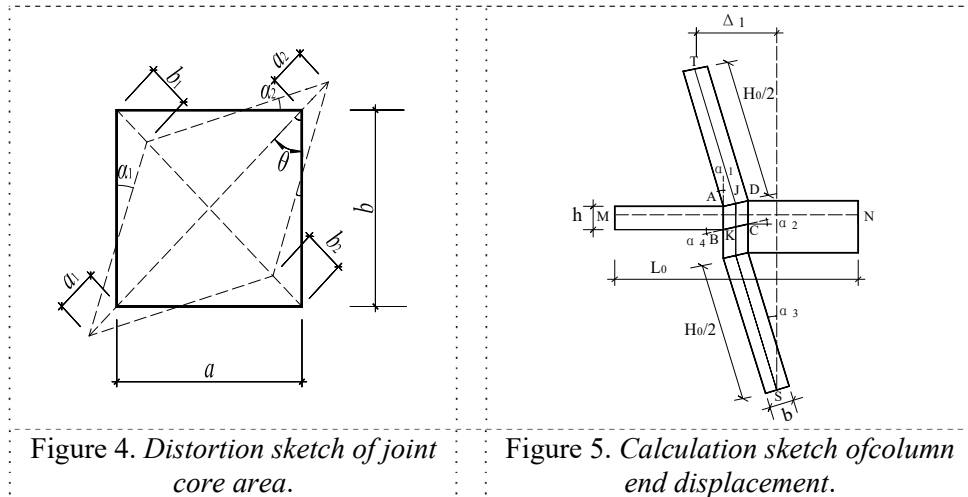


Figure 4. Distortion sketch of joint core area.

Figure 5. Calculation sketch of column end displacement.

As shown in the fig.6,  $P-\Delta_1$  hysteretic curves of all the specimens are very plump. The ultimate horizontal displacement on the top of all columns caused by shear deformation in the small core are more than 60 mm. Contrast from  $P-\Delta$  curves and  $P-\Delta_1$  curves, which can be seen that the small core area of the joint has stronger energy dissipation capacity. Moreover, energy dissipation in the small core area occupy most of the total energy consumption of the specimens.

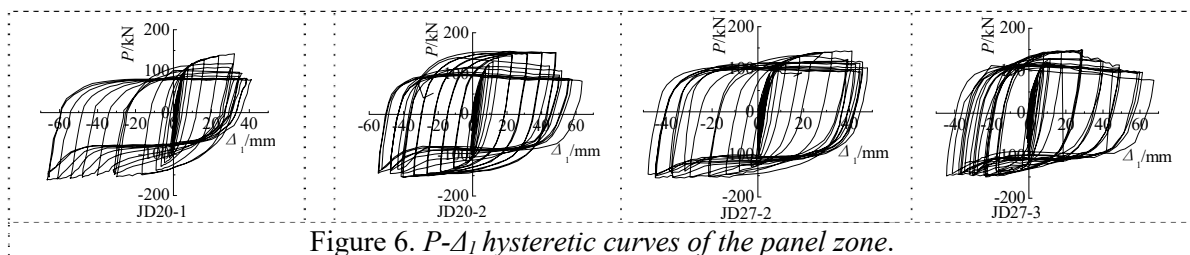


Figure 6.  $P-\Delta_1$  hysteretic curves of the panel zone.

#### 4.2 Energy dissipation of panel zone

The graphic area of load-displacement hysteresis curve under the action of repeated load is commonly used to measure the energy dissipation of the joint[10]. In the  $P-\Delta_1$  hysteresis curve, the sum of unloading curve area and loading curve area is the energy dissipation of the panel zone. Accordingly, the equivalent viscous damping coefficient  $\zeta_{eq}$  and the energy dissipation coefficient  $D_e$  defined by Specification for Building Seismic Test Method (JGJ101—96) are used to evaluate energy dissipation capacity of the panel zone. The equivalent viscous damping coefficient  $\zeta_{eq}$  and the energy dissipation coefficient  $D_e$  in each stage are shown in table 3. Where,  $\Delta_s$ ,  $\Delta_m$  and  $\Delta_u$  respectively is deformation on the top of column in the yield stage of the panel zone, the limit stage of the panel zone and the failure stage of the panel zone.  $\theta_p$  is plastic rotation angle of the panel zone[11].

The table 3 shows that the equivalent viscous damping coefficient and the energy dissipation coefficient of all joints increases with the increase of plastic rotation angle of the panel zone. This illustrates that energy dissipation ability of the joint gradually increases with the increase of the shear

deformation of joint core area. When the plastic rotation angle stands at about 0.018, all specimens has reached the ultimate bearing capacity. Since then, the equivalent viscous damping coefficient and the energy dissipation coefficient of panel zone have still risen in a certain way with the increase of plastic deformation of the panel zone (shown in fig.7). In short, all joints have good ductility and deformation capacity at the later stage. After the destruction of all joints, the equivalent viscous damping coefficient is between 0.38 and 0.45, energy dissipation coefficient is between 2.46 and 2.86. Which illustrates that the energy dissipation capacity of steel irregular joint is very close to the energy dissipation capacity of normal steel joint. This shows that this kind of joint has good seismic performance and energy dissipation capacity.

Table 3. The equivalent viscous damping coefficient and the energy dissipation coefficient.

Joint Number	Stage	$\theta_p$	$\zeta_{eq}$	$D_e$
JD20-1	$\Delta_s$	0.0016	0.1481	0.9303
	$\Delta_m$	0.0228	0.3904	2.4518
	$\Delta_u$	0.0245	0.3953	2.5132
JD20-2	$\Delta_s$	0.0025	0.1227	0.7707
	$\Delta_m$	0.0203	0.3663	2.3004
	$\Delta_u$	0.0250	0.4127	2.7438
JD20-3	$\Delta_s$	0.0022	0.1568	0.9848
	$\Delta_m$	0.0176	0.3732	2.3438
	$\Delta_u$	0.0205	0.3829	2.4673
JD27-2	$\Delta_s$	0.0019	0.1620	1.0176
	$\Delta_m$	0.0173	0.3677	2.3092
	$\Delta_u$	0.0195	0.4209	2.7855
JD27-3	$\Delta_s$	0.0022	0.1348	0.8465
	$\Delta_m$	0.0187	0.4263	2.6769
	$\Delta_u$	0.0260	0.4537	2.8633

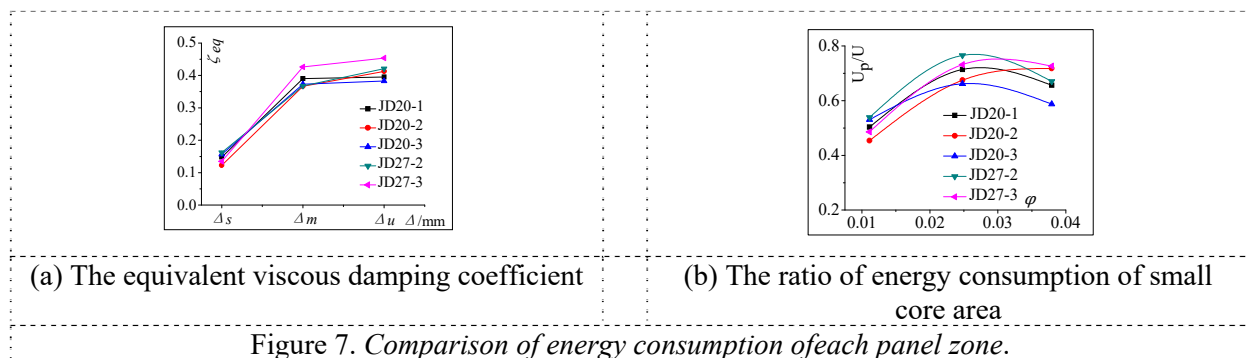


Figure 7. Comparison of energy consumption of each panel zone.

As shown in the fig.7 (b), the energy dissipation coefficient of the small core area reaches the maximum when displacement angle is about 0.025. The energy dissipation of the small core area accounts for 70% of the total energy dissipation of the joint. When the displacement angle has been continuing to increase, the panel zone has completely gotten into plastic stage. At this moment, the energy dissipation of the small core area as a proportion of the total energy dissipation of specimens fell gradually.

## 5. Conclusions

Based on the experimental and theoretical study results, the conclusions summarized are as follows:

- The total energy dissipation of the specimens consists of three parts, namely energy dissipation of the panel zone, energy dissipation of the beam plastic hinge, and energy dissipation of the column plastic hinge. The test data and test phenomenon show that the plastic shear deformation of small core area is much greater than 2nd zone. The results indicate that energy dissipation in the small core area of panel zone plays key roles in energy dissipation of the specimen.

- The displacement ductility coefficient  $\mu$  of six joint specimens is 2.02 between 2.66, with a mean of 2.29. The displacement ductility coefficients of six joint specimens is not very big. The reason is that bearing capacity drops rapidly because of sudden fracture of the weld between steel column flange and connection web under the action of repeated horizontal load after the web of joint core area yield. Therefore, the weld quality of the panel zone is highly valued.

- Energy dissipation in the small core area of the panel zone plays key roles in energy dissipation for the specimen. The plastic rotation angle of the panel zone is 0.017 between 0.023 under the ultimate loading. After the destruction of all joints, the equivalent viscous damping coefficient is between 0.38 and 0.45, energy dissipation coefficient is between 2.46 and 2.86. Which illustrates that that this kind of joint has good seismic performance and energy dissipation capacity.

### Acknowledgments

The financial assistance is provided by the Natural Science Foundation of China No. 51308444 and the Postdoctoral Science Foundation of China No. 20080440814. These supports are gratefully acknowledged.

### References

- [1] Popov E. P., Pinkney R. B. (1978) Seismic moment connections for MRFs. *Journal of the Structural Division*, 10(1-4):163-198.
- [2] Krawinkler H., Popov E. P. (1982) Seismic behavior of moment connections and joints. *Journal of the Structural Division*, 108(ST2):373-391.
- [3] Krawinkler H. (2003) Shear in beam - column joints in seismic design of steel frames. *Engineering Journal*, 66(1):82-91.
- [4] Mulas M. G. (2004) A structural model for panel zones in nonlinear seismic analysis of steel moment-resisting frames. *Engineering Structures*, 26(2):363-380.
- [5] Hu Z. B. (2010) Experimental and theoretical research on performance of irregular joint between steel box columns and beams. Xi'an University of Architecture and Technology, Xi'an. pp. 24-27. (in Chinese)
- [6] Japan Steel Construction Society. (2003) Overview of steel structure technology. China Building Industry Press, Beijing. pp. 265-270.
- [7] Xue J. Y., Hu Z. B., Peng X. N., Liu Z. Q. (2011) Analysis of shear resistance of irregular joint between steel box columns and beams. *Civil Engineering Journal*, 44(8):9-15. (in Chinese)
- [8] Wardenier J. (2002) Hollow Section in Structural Applications. John Wiley & Sons, NewYork. pp. 75-80.
- [9] Chen S. F. (1998) Principles of steel structure design. Science and Technology Press, Beijing. pp. 188-189. (in Chinese)
- [10] Fielding D. J., Huang J. S. (1971) Shear in steel beam-to-column connections. *The Welding Journal*, 50(7):1-10.
- [11] Wang W. Z. (2003) Fracture mechanism, cyclical performance and design recommendations of welded flange-bolted web beam-to-column rigid connections in steel moment frames under seismic load. Xi'an University of Architecture and Technology, Xi'an. pp. 82-84. (in Chinese)